

Entanglement in Quantum Phase Transitions with Two- and Three-body Interactions

Xinhua Peng^{1,2,*}, Jingfu Zhang², Jiangfeng Du¹, and Dieter Suter^{2†}

¹Hefei National Laboratory for Physical Sciences at Microscale and Department of Modern Physics, University of Science and Technology of China, Hefei, Anhui 230026, People's Republic of China and

²Fakultät Physik, Technische Universität Dortmund, 44221 Dortmund, Germany

(Dated: February 25, 2019)

Quantum phase transitions describe qualitative changes in the ground state of many-body systems driven solely by quantum fluctuations. In a system of three spins subject to one-, two- and three-body interactions, the quantum mechanical ground state can be a product state or one of different entangled states, including W- and GHZ states. We discuss the relevant phase diagram and realize the system experimentally in an NMR quantum simulator, where we generate the relevant Hamiltonian and drive the system through different critical points by adiabatically changing a suitable control parameter.

PACS numbers: 03.67.-a, 03.65.Ud, 03.67.Mn

Introduction. – At absolute zero temperature, a system can undergo a quantum phase transition (QPT) to a new ground state as a result of a change in one of the parameters of the Hamiltonian [1]. Well-known examples are the superconductor-insulator transition and the paramagnetic-antiferromagnetic transition in quantum magnets. QPTs were experimentally observed in magnetic systems [2], heavy-fermion metals [3], common metals [4] and Bose-Einstein condensation [5]. Also, the investigation of such phase transitions often leads to the discovery of novel materials. A collection of reviews [6] on the topic of QPTs reported the current status and recent developments in this field.

QPTs are associated with a system of interacting particles; depending on the control parameters of the relevant Hamiltonian, its ground state may be a product state or an entangled state. For some QPTs, entanglement is therefore a useful order parameter [7]. An example of such a quantum critical point that separates a product state from a maximally entangled state has been experimentally observed for a two-qubit Heisenberg spin chain [8, 9].

In most systems studied, attention was focused on two-body interactions, which are most readily accessible experimentally. On the other hand, spin systems with three-spin interactions have attracted a lot of interest, since they may exhibit exotic ground-state properties, including topological phases or spin liquids [10], incommensurate phases [11], and chiral phase transitions [12]. Effective three-body interactions have been found in cold polar molecules [13] or atoms in optical lattices [14].

In this Letter, we study the ground-state properties of spin chains with both Ising-type two-spin interactions and three-spin interactions, which can show distinct quantum phases with qualitatively different types of entanglement or no entanglement at all. For a three-spin system, we discuss the complete phase diagram, which includes differently entangled ground states. Using suitable adiabatic variations of the control parameters,

we drive the system through different quantum critical points, from a product state to one of the entangled states (including GHZ and W states) in an NMR quantum simulator. The resulting states are characterized by suitable entanglement witnesses [15, 16] and further verified by quantum state tomography.

System. – Consider a closed 1D spin-chain in a uniform magnetic field, which consists of spins 1/2 interacting by both Ising-type nearest-neighbor two-body and three-body couplings:

$$\mathcal{H} = \omega_z \sum_i \sigma_z^i + \omega_x \sum_i \sigma_x^i + J_2 \sum_i \sigma_z^i \sigma_z^{i+1} + J_3 \sum_i \sigma_z^i \sigma_z^{i+1} \sigma_z^{i+2}, \quad (1)$$

where the σ_z^i are the Pauli operators, ω_z and ω_x the strengths of the longitudinal and transverse magnetic fields, and J_2 , J_3 the two-spin and three-spin coupling constants. The transverse field is small, $|\omega_x| \ll 1$, and we assume periodic boundary conditions, $\sigma_z^{N+i} = \sigma_z^i$.

Here, we discuss the simplest case of three spins. Since the Hamiltonian is symmetric with respect to permutation of the qubits, we choose a symmetry-adapted basis. The totally symmetric subspace is spanned by the states $|000\rangle$, $|W_{001}\rangle$, $|W_{110}\rangle$, and $|111\rangle$, where the W states are

$$\begin{aligned} |W_{001}\rangle &= \frac{1}{\sqrt{3}} (|001\rangle + |010\rangle + |100\rangle) \\ |W_{110}\rangle &= \frac{1}{\sqrt{3}} (|110\rangle + |101\rangle + |011\rangle). \end{aligned} \quad (2)$$

The W states represent genuine tripartite entanglement and can retain maximal bipartite entanglement when any one of the three qubits is traced out [17]. Using perturbation theory in this subspace, we find its ground state as a function of the three control parameters ω_z , J_2 , and J_3 . Table I summarizes the different phases for the half-space $\omega_z \geq 0$. Similar expressions are obtained for $\omega_z < 0$. As usual, the Greenberger-Horne-Zeilinger (GHZ) state is defined as $|\text{GHZ}_\pm\rangle = (|000\rangle \pm |111\rangle)/\sqrt{2}$. Its local transform is $|\overline{\text{GHZ}}_\pm\rangle$ by three local Hardarmard gates. Like

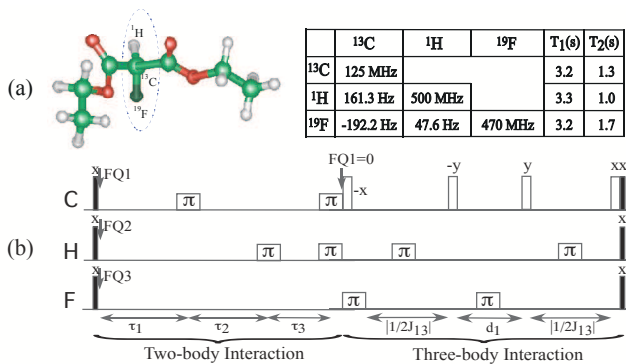


FIG. 2: (Color Online) (a) Molecular structure and properties of the quantum register: Diethyl-fluoromalonate. The oval marks the three spins used as qubits. The table on the right summarizes the relevant NMR parameters measured at room temperature on a Bruker Avance II 500 MHz (11.7 Tesla) spectrometer, i.e. the Larmor frequencies ω_i (on the diagonal), the J-coupling constants J_{ij} (below the diagonal), and the relaxation times T_1 and T_2 in the last two columns. (b) Pulse sequence for simulating the Hamiltonian of Eq. (1). The narrow black rectangles represent small-angle rotations, the narrow empty rectangles denote 90° rotations and the wide ones denote the refocusing 180° pulses. The delays are $\tau_i = J_2\tau/[1/(\pi J_{ij}) + 1/(\pi J_{jk})]$ with (i, j, k) an even permutation of $(1, 2, 3)$ and $d_1 = 2J_3\tau/(\pi J_{12})$. The offsets between the irradiation frequencies and their Larmor frequencies are $FQ1 = 2\omega_z\tau/(\tau_1 - \tau_2 + 3\tau_3)$, $FQ2 = 2\omega_z\tau/(\tau_1 + \tau_2 - \tau_3)$ and $FQ3 = 2\omega_z\tau/(\tau_1 + \tau_2 + \tau_3)$.

T is the total duration of the adiabatic passage and C is the control parameter in $\mathcal{H}(t)$. The adiabatic condition is achieved when both $T, M \rightarrow \infty$ and the duration of each step $\tau \rightarrow 0$.

To observe the different types of phase transitions in the Hamiltonian (1), we chose two different parameter subspaces: Case (A): Phase transition from a product state to a W entangled state: the control parameter is the two-spin coupling strength J_2 from $J_2(0) = 0$ to $J_2(T) = 2$ when $\omega_z = -2$, $\omega_x = 0.09$ and $J_3 = 0$, as shown in Fig. 1 (c); Case (B) Phase transition from a product state to a GHZ entangled state: the control parameter is the three-spin coupling strength J_3 from $J_3(0) = 0$ to $J_3(T) = 2$ when $\omega_z = J_2 = 0$ and $\omega_x = 0.12$, as shown in Fig. 1 (d). We used a hyperbolic sine for the variation of the control parameters J_2 and J_3 in the experiments [9].

The system was first initialized in the ground state of the initial Hamiltonian $\mathcal{H}(0)$ for Case (A) by preparing a pseudo-pure state (PPS) $\rho_{000} = (1 - \epsilon)\mathbf{1}/8 + \epsilon|000\rangle\langle 000|$ using spatial averaging techniques [23]. Here $\mathbf{1}$ represents the unity operator and $\epsilon \approx 10^{-5}$ the thermal polarization. For Case (B), the initial state $(1/\sqrt{8})(|0\rangle - |1\rangle)^{\otimes 3}$ was prepared by applying $\pi/2$ pulses along the $-y$ axis to each qubit of the state ρ_{000} . Then, the adiabatic evolution for each case was performed from the corresponding initial state.

Quantum phase transition and entanglement witness.

– In order to detect the presence of the multipartite entanglement, we used the method of entanglement witnesses [16]. These witness operators can always be used to detect various forms of multipartite entanglement, provided we have some *a priori* knowledge about the states under investigation.

A witness operator has the canonical form $\mathcal{W}_d = \alpha\mathbf{1} - \mathcal{Q}$, where \mathcal{Q} is a projection operator [15]. Table II lists some witness operators that are suitable for detecting different types of multipartite entanglement for a three-qubit state ρ [16].

TABLE II: Witness operators for detecting multipartite entanglement of the three-qubit state ρ . The set of all three-qubit states include S: separable class; B: biseparable class; W class and GHZ class. Here the GHZ witness is $\mathcal{W}_{\text{GHZ}} = \frac{3}{2}\mathbf{1} - |\text{GHZ}_-\rangle\langle \text{GHZ}_-|$ and the two W witnesses are $\mathcal{W}_{\text{W}_1} = \frac{4}{3}\mathbf{1} - |\text{W}_{001}\rangle\langle \text{W}_{001}|$ and $\mathcal{W}_{\text{W}_2} = \frac{1}{2}\mathbf{1} - |\text{GHZ}_-\rangle\langle \text{GHZ}_-|$.

\mathcal{W}_d	\mathcal{W}_{GHZ}		\mathcal{W}_{W_1}		\mathcal{W}_{W_2}		
$\text{Tr}(\rho\mathcal{W}_d)$	≥ 0	< 0	≥ 0	< 0	≥ 0	$[0, -1/4]$	$\leq -1/4$
Class	W, B, S	GHZ	B, S	GHZ W	B, S	GHZ W	GHZ

The key part in these witness operators is the projective measurement of the positive operator \mathcal{Q} ($= |\text{GHZ}_-\rangle\langle \text{GHZ}_-|$ or $|\text{W}_{001}\rangle\langle \text{W}_{001}|$), which was transformed into the computational basis for the measurements [24]. Taking into account the effect of decoherence, the experimental signals were first corrected by an effective decoherence time T_2^{eff} , which was estimated by fitting the decay of the signal with the duration of the experiment. The experimental results are shown in Fig. 3, which indicates the generation of a W state as the strength J_2 of the two-spin interaction increases, i.e., $\langle \mathcal{W}_{\text{GHZ}} \rangle > 0$, $\langle \mathcal{W}_{\text{W}_2} \rangle > 0$ and $\langle \mathcal{W}_{\text{W}_1} \rangle < 0$ after the critical point $J_2 = 1$. Conversely, we observe the generation of a GHZ state if the strength J_3 of the three-spin interaction increases, i.e., $\langle \mathcal{W}_{\text{GHZ}} \rangle < 0$, $\langle \mathcal{W}_{\text{W}_2} \rangle < -1/4$ and $\langle \mathcal{W}_{\text{W}_1} \rangle > 0$ when $J_3 \gg 0$.

We also confirmed these results by performing complete quantum state tomography [25] at the end of the adiabatic evolution, shown in Fig. 4. The fidelities of our states ρ_{exp} with the ideal states $|\psi_{id}\rangle$: $F = |\langle \psi_{id} | \rho_{\text{exp}} | \psi_{id} \rangle|$ are 0.61 for the W state and 0.73 for the GHZ state. The low fidelity mainly results from relaxation during the long adiabatic passage, about 146 ms for Case (A) and 62 ms for Case (B). If we used the experimental fidelity $F = |\langle \psi_{id} | \rho_{\text{exp}} | \psi_{id} \rangle| / \text{Tr}(\rho_{\text{exp}}^2)$, this yielded $F(\rho_{\text{exp}}^{\text{W}}) = 0.90$ and $F(\rho_{\text{exp}}^{\text{GHZ}}) = 0.92$, which provide quantitative confirmation.

Conclusion. – To summarize, we have discussed the rich variety of quantum phases in a triangular Heisenberg spin chain. Two inequivalent ways of entangling three

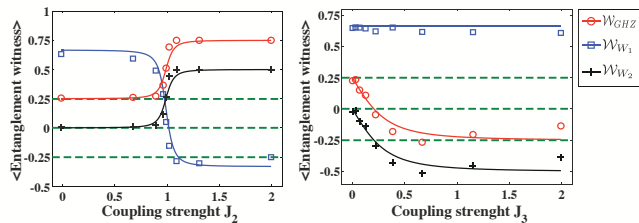


FIG. 3: (Color Online) Experimental entanglement detection using the witness operators \mathcal{W}_{GHZ} , \mathcal{W}_{W_1} and \mathcal{W}_{W_2} for Case (A) (left part) and Case (B) (right part), indicating the change of the ground state at the critical point. Here the effective decoherence time T_2^{eff} was estimated as 150 ms for (A) and 600ms for (B). Solid lines represent the theoretical expectation.

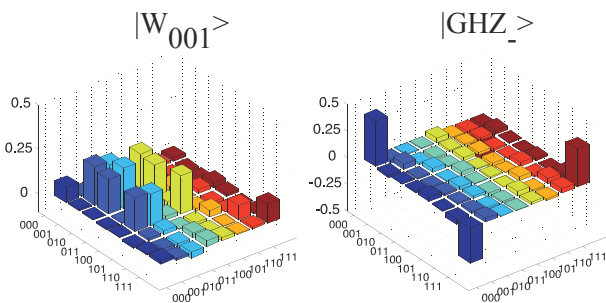


FIG. 4: (Color online) Real part of the density matrices for the W state generated by two-spin interactions, and the GHZ state generated by the three-spin interaction. The rows and columns represent the standard computational basis in binary order, from $|000\rangle$ to $|111\rangle$. We applied a Hadamard-transform to the real ground state of Case (B) to give a cleaner signature of the GHZ state.

qubits, represented by the GHZ state and the W state, appear with the competition among two-spin, three-spin and the Zeeman interactions. Using an NMR quantum simulator, we have experimentally confirmed that the system ground state undergoes a QPT from a classical product state to multipartite entangled states (W state or GHZ state) when this system is swept adiabatically through the relevant parameter space by properly varying a Hamiltonian parameter. The presence of multipartite entanglement was characterized by two methods: entanglement witnesses and quantum state tomography.

We expect even more fascinating new phases in multi-qubit systems beyond three qubits, since these qubits can be entangled in more inequivalent ways, e.g., nine ways for four qubits [26]. However, the characterization of multi-qubit entanglement is very complex. The identification, classification and quantification of multipartite entanglement for pure and mixed states beyond three-qubit systems remains an unsolved issue.

This work is supported by the DFG through Su 192/19-1, NNSFC, the CAS and the Alexander von Humboldt Foundation.

* Electronic address: xhpeng@ustc.edu.cn

† Electronic address: Dieter.Suter@tu-dortmund.de

- [1] S. Sachdev, *Quantum Phase Transition* (Cambridge University Press, Cambridge, 1999); P. Coleman and A. J. Schofield, *Nature* **433**, 226 (2005).
- [2] H. M. Rønnow *et al.*, *Nature* **424**, 524 (2003);
- [3] J. Custers *et al.*, *Nature* **424**, 524 (2003); M. Neumann *et al.*, *Science* **317**, 1356 (2007); P. Gegenwart *et al.*, *ibid.* **315**, 969 (2007).
- [4] A. Yeh *et al.*, *Nature* **419**, 459 (2002).
- [5] M. Greiner *et al.*, *Nature* **415**, 39 (2002); S. E. Sebastian *et al.*, *ibid.* **441**, 617 (2006).
- [6] P. C. Canfield, *Nature Phys.* **4**, 167 (2008); D. M. Broun, *ibid.* **4**, 170 (2008); S. Sachdev, *ibid.* **4**, 173 (2008); P. Gegenwart *et al.*, *ibid.* **4**, 186 (2008); T. Giamarchi *et al.*, *ibid.* **4**, 198 (2008).
- [7] A. Osterloh *et al.*, *Nature* **416**, 608 (2002); G. Vidal *et al.*, *Phys. Rev. Lett.* **90**, 227902 (2003); F. Verstraete *et al.*, *ibid.* **92**, 027901 (2004); J. Latorre *et al.*, *Quant. Inf. Comput.* **4**, 48 (2002);
- [8] J. Zhang *et al.*, *Phys. Rev. Lett.* **100**, 100501 (2008).
- [9] X. Peng *et al.*, *Phys. Rev. A* **71**, 012307 (2005).
- [10] N. R. Cooper, *Phys. Rev. Lett.* **92**, 220405 (2004); O. I. Motrunich and T. Senthil, *ibid.* **89**, 277004 (2002); Y. Kurosaki *et al.*, *ibid.* **95**, 177001 (2005);
- [11] H. Frahm, *J. Phys. A* **25**, 1417 (1992); A. M. Tsvelik, *Phys. Rev. B* **42**, 779 (1990).
- [12] C. D’Cruz and J. K. Pachos, *Phys. Rev. A* **72**, 043608 (2005); I. Dimitris *et al.*, *ibid.* **77**, 012106 (2008).
- [13] H. P. Büchler *et al.*, *Nature Phys.* **3**, 726 (2007).
- [14] J. K. Pachos and E. Rico, *Phys. Rev. A* **70**, 053620 (2004); J. K. Pachos and M. B. Plenio, *Phys. Rev. Lett.* **93**, 056402 (2004).
- [15] A. Sanpera *et al.*, *Phys. Rev. A* **63**, 050301(R) (2001); M. Lewenstein *et al.*, *Phys. Rev. A* **62**, 052310 (2000).
- [16] M. Bourennane *et al.*, *Phys. Rev. Lett.* **92**, 087902 (2004); A. Acín *et al.*, *ibid.* **87**, 040401 (2001); M. Horodecki *et al.*, *Phys. Lett. A* **223**, 1 (1996).
- [17] W. Dür, G. Vidal, and J. I. Cirac, *Phys. Rev. A* **62**, 062314 (2000).
- [18] N. Linden *et al.*, *Chem. Phys. Lett.* **305**, 28 (1999); J. A. Jones and E. Knill, *J. Mag. Res.* **141**, 322 (1999).
- [19] C. H. Tseng *et al.*, *Phys. Rev. A* **61**, 012302 (1999).
- [20] A. Messiah, *Quantum Mechanics* (Wiley, New York, 1976).
- [21] R. P. Feynman, *Int. J. Theor. Phys.* **21**, 467 (1982).
- [22] M. Steffen *et al.*, *Phys. Rev. Lett.* **90**, 067903 (2003).
- [23] D. G. Cory *et al.*, *Physica D* **120**, 82 (1998); N. A. Gershenfeld and I. L. Chuang, *Science* **275**, 350 (1997).
- [24] G. Brassard *et al.*, *Phys. D* **120**, 43 (1998).
- [25] I. L. Chuang *et al.*, *Proc. R. Soc. Lond. A* **454**, 447 (1998); G. M. Leskowitz and L. J. Mueller, *Phys. Rev. A* **69**, 052302 (2004).
- [26] F. Verstraete *et al.*, *Phys. Rev. A* **65**, 052112 (2002).